

## Photoluminescence and radiation effect of Er and Pr implanted silicon-rich silicon oxide thin films

Fang Zhu<sup>a</sup>, Zhisong Xiao<sup>a,\*</sup>, Lu Yan<sup>a</sup>, Feng Zhang<sup>a</sup>, Kun Zhong<sup>b</sup>, Guoan Cheng<sup>b</sup>

<sup>a</sup> Department of Physics, School of Science, Beihang University, Beijing 100191, China

<sup>b</sup> Department of Materials Science and Engineering, Beijing Normal University, Beijing 100875, China

### ARTICLE INFO

#### Article history:

Available online 16 June 2009

#### PACS:

78.55.Hx

#### Keywords:

Er  
Pr  
Si/SiO<sub>2</sub>  
Photoluminescence  
Energy transfer

### ABSTRACT

Er and Pr ions were implanted into silicon-rich silicon oxide (SRSO) thin films with Si crystals embedded in SiO<sub>2</sub> matrix. The 525 and 546 nm luminescence peaks were clearly observed in Er-only doped film, but disappeared in the photoluminescence (PL) spectra of Er–Pr codoped films. Instead, a broad PL spectrum extending from 450 to 700 nm was obtained for Er–Pr codoped films with Er/Pr concentration ratio of 1. Concentration profiles of Si, Er and Pr ions in films were simulated by SRIM2006 and related radiation effect on PL response was also discussed. Our results indicate that this material is a potential candidate for the development of white light-emitting diode (LED) and field emission displays for its visible luminescence.

Crown Copyright © 2009 Published by Elsevier B.V. All rights reserved.

### 1. Introduction

Considerable research has been focused on the visible light emitting using rare earth (RE) ions such as Er<sup>3+</sup>, Pr<sup>3+</sup>, Eu<sup>3+</sup>, Nd<sup>3+</sup>, Ho<sup>3+</sup> and Tm<sup>3+</sup> doping in different hosts in the past decades [1–4]. White light source with high emissivity is required for display and lighting technology, which can be generated either by precise mixing of primary colors, i.e. blue, green, and red colors or by light with complementary colors. Efforts to simulate the white light emission by controlling the intensities of different red–green–blue (RGB) lights have been reported by researchers using RE ions doped in different lattices. Silva et al. obtained white light in Tm/Er/Yb codoped fluoride glasses [5]. Recently Gouveia et al. demonstrated white emission in Tm/Ho/Yb codoped fluorolead germinate glass with high color purity (blue: 97%; green: 100%; red: 95%) [6].

Among those RE ions, Er<sup>3+</sup> is the most popular one due to its large efficiency in the region of prime colors. Pr<sup>3+</sup> has also been found much attractive as it offers the efficient IR emission for optical amplification at 1.3 μm and RGB emission simultaneously [7,8]. To improve the luminescence efficiency, RE ions have been implanted in silicon-rich silicon oxide (SRSO) thin films. A particular advantage of RE ions doped in SRSO thin films is that the excitation of RE ions occurs predominantly through an Auger-type interaction between carriers in nc-Si and the RE ions [9]. Si nano-crystalline

(nc-Si) were demonstrated to act as photosensitizers for molecular oxygen and several kinds of rare earth ions. In particular, erbium ions can be excited very efficiently by the energy transfer from nc-Si. The effective absorption cross-section of the intra-4f shell transition of Er<sup>3+</sup> was enhanced by 2–4 orders of magnitude because of the large absorption cross-section of nc-Si in visible range and high efficient energy transfer from nc-Si to Er<sup>3+</sup> [10].

In the present work we have demonstrated the generation of violet–green–red emission from a combination of Er–Pr codoped in SRSO thin film. Concentration profiles of Si, Er and Pr ions in films were simulated by the SRIM2006 and related radiation effect on PL response was also discussed.

### 2. Experiment

Wet oxygen oxidation was performed to produce SiO<sub>2</sub> film on Si(1 0 0) wafers at 1000 °C for 1.5 h. The thickness of resultant SiO<sub>2</sub> film was more than 1 μm, which was calculated by silicon oxidation dynamics formulation. SiO<sub>2</sub> films were implanted in vacuum with  $3 \times 10^{17} \text{ cm}^{-2}$  Si ions at 45 keV by using a metal vapor vacuum arc (MAVVA) implanter. Then  $2 \times 10^{16} \text{ cm}^{-2}$  Er ions were implanted at 60 keV. Finally, Pr ions were implanted with ion dose of 2, 4, 8, 10 and  $20 \times 10^{16} \text{ cm}^{-2}$  at 60 keV. The resulting Pr peak concentration was varied from  $2 \times 10^{20}$  to  $2 \times 10^{21} \text{ cm}^{-3}$ . The ion beams were implanted with an incident angle of ~10° with respect to the substrate in order to minimize ion-channeling effects. The implanted samples were then annealed in air for 2 h at 800 °C.

\* Corresponding author.

E-mail address: [zsxiao@buaa.edu.cn](mailto:zsxiao@buaa.edu.cn) (Z. Xiao).

The annealed sample implanted with only Si ions was analyzed by X-ray diffraction (XRD) using a  $\theta - 2\theta$  diffractometer excited with a Cu  $K\alpha$  I ( $\lambda = 0.15406$  nm) radiation as well as a step size of  $0.02^\circ$ . Photoluminescence (PL) of the samples was measured using a fluorescence photospectrometer at room temperature. The PL signal was detected by CCD detector. All spectra were excited at the wavelength of 325 nm.

### 3. Results and discussion

Si ions were implanted into  $\alpha$ -SiO<sub>2</sub> thin films followed by 800 °C annealing. Crystalline (1 1 1) Si (c-Si) was formed as shown in XRD spectrum (Fig. 1). Nano-crystalline Si (nc-Si) is also possibly existed in those films as reported by Xiao et al. [11]. The introduced c-Si provided the system with a large absorption cross-section ( $10^{-16}$ – $10^{-17}$  cm<sup>2</sup>) and acted as sensitizers for the RE ions. This excitation process has been modeled as a dipole–dipole interaction between the c-Si (nc-Si) and Er<sup>3+</sup> with characteristic energy transfer times less than 1  $\mu$ s [12]. Kik et al. reported that the maximum activated Er<sup>3+</sup> concentration by Si nanocrystals was of about  $1 \times 10^{19}$  cm<sup>-3</sup> for the samples annealed at high temperature (1100 °C). They attributed such saturation to Er clustering effect or to Auger deexcitation [13]. More recently, Wojdak et al. found that in highly doped samples ( $[Er] = 2 \times 10^{20}$  cm<sup>-3</sup>) the activated Er<sup>3+</sup> fraction was less than 3%. Franzò et al. observed an enhanced Er<sup>3+</sup> emission by reducing processing temperature of Er-doped SRSO to 800 °C. In this case there are amorphous Si nanoclusters in the processed layers, which appear to act as better Er-sensitizing centers than the crystalline Si by showing a larger density and a concomitant reduction of the relative distance between Er ions and nc-Si [14].

Fig. 2 shows the luminescence of Er-only doped SRSO film. The green emission at 525 and 546 nm is originated from the Er<sup>3+</sup>  ${}^2H_{11/2} \rightarrow {}^4I_{15/2}$  and  ${}^4S_{3/2} \rightarrow {}^4I_{15/2}$  transition, respectively. The red PL peak at 662 nm is due to the  ${}^4F_{9/2} \rightarrow {}^4I_{15/2}$  transition of Er<sup>3+</sup>. There are also 380 nm violet PL peak and near infrared 769 nm emission due to  ${}^2H_{9/2} \rightarrow {}^4I_{15/2}$  and  ${}^4I_{9/2} \rightarrow {}^4I_{15/2}$  transition, respectively. The broad emission band ranging from 450 to 700 nm is proposed to be the contribution of amorphous and c-Si (nc-Si) luminescence in SiO<sub>2</sub> matrix. The peak of this broad PL band may shift from sample to sample, depending on the band gap (related to the size) of nc-Si. Liu et al. observed the peak shift from 590 nm (for a 700 °C annealed sample) to 750 nm (for an 1100 °C annealed sample) [15].

Fig. 3 shows the PL spectra of Er–Pr codoped SRSO films. Comparing with the PL spectra of Er-only doped film, the broad lumi-

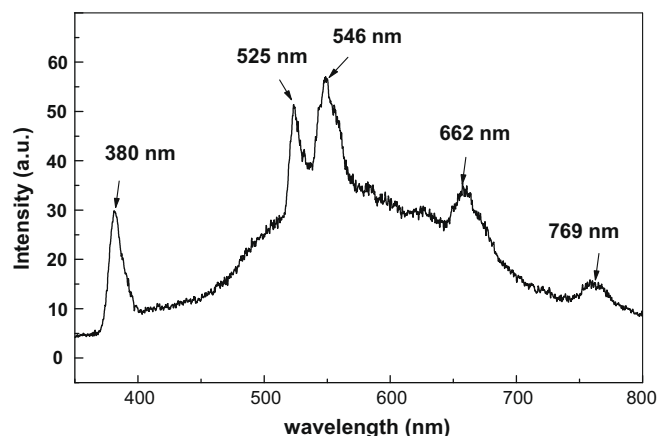


Fig. 2. PL spectra of Er-only doped SRSO film.

nescence band of 450–700 nm was clear for the film with Pr/Er concentration ratio of 1 (Pr ion dose of  $2 \times 10^{16}$  cm<sup>-2</sup>). A new green emission peak at 568 nm is originated from Pr<sup>3+</sup>  ${}^3P_1 \rightarrow {}^3H_5$  transition and the red emission of 618 nm is due to Pr<sup>3+</sup>  ${}^3P_1 \rightarrow {}^3H_6$  transition. The shoulder PL peak is locating at  $\sim$ 500 nm is suggested to be the transition of Pr<sup>3+</sup> from  ${}^3I_0 + {}^3P_1$  state to  ${}^3H_4$  or  ${}^3H_5$  state. By Pr codoping the Er<sup>3+</sup> emission at 525, 546 and 662 nm disappeared or overlapped by the broad luminescence band of 450–700 nm. Instead, Pr<sup>3+</sup> emission at 495, 568 and 618 nm were observed. It could be understood by the energy transfer process from Er<sup>3+</sup> to Pr<sup>3+</sup> as following.

After absorption of the pumping photons Er<sup>3+</sup> rapidly relaxed into  ${}^2H_{11/2}$ ,  ${}^4S_{3/2}$  and  ${}^4F_{9/2}$  state through nonradiative processes, which have been indicated in [5]. The Pr ions after absorption of the pumping photons could relax to  ${}^3F_4$  state by a nonradiative transition, and then relaxed the ground state, corresponding to the well known 1.3  $\mu$ m emission [7]. The Er<sup>3+</sup>  ${}^4F_{9/2} \rightarrow {}^4I_{15/2}$  transition is nearly resonant with the Pr<sup>3+</sup>  ${}^3F_4 \rightarrow {}^3P_2$  transition with an energy mismatch less than 0.1 eV. The energy levels involved for observed PL bands of Er<sup>3+</sup> ion and related transitions are depicted in Fig. 4. Finally, the Pr<sup>3+</sup> ions decayed nonradiatively from the  ${}^3P_2$  state back to the  ${}^3P_1$  nearly instantaneously, since the multiphonon effects in silica would result in a nonradiative Pr<sup>3+</sup>  ${}^3P_2 \rightarrow {}^3P_1$  transition at a much fast rate, which enhanced the emission of Pr<sup>3+</sup> 568 and 618 nm. We simulated concentration profiles of Si, Er and Pr ions and introduced vacancies in films by SRIM2006. Fig. 5 shows that Er ions and Pr ions located in the same range

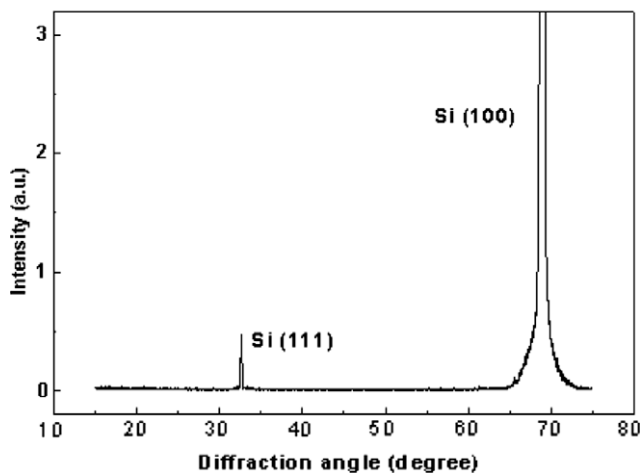


Fig. 1. XRD spectrum of SiO<sub>2</sub> sample implanted with only Si.

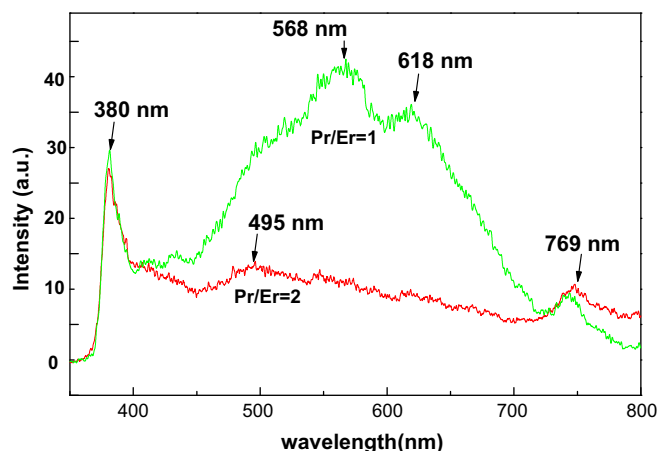


Fig. 3. PL spectra of Er–Pr codoped SRSO film with  $[Er]/[Pr]$  concentration ratio of 1.

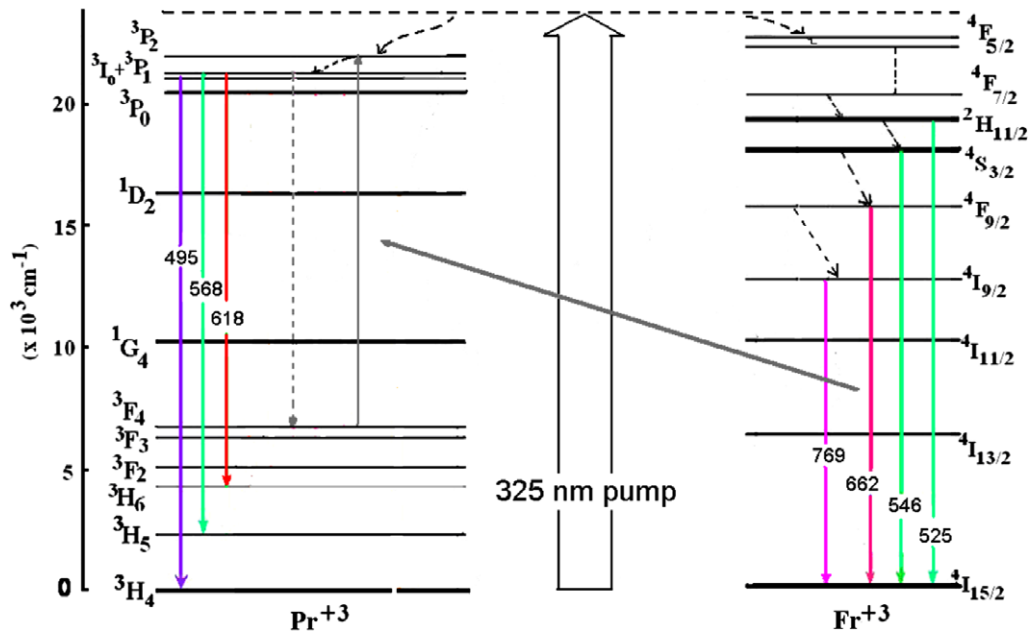


Fig. 4. Schematic energy level diagram of  $\text{Er}^{3+}$  and  $\text{Pr}^{3+}$  showing different transitions in Er–Pr codoped SRSO films.

$80 \pm 50$  nm under surface. Since  $\text{Pr}^{3+}$  and  $\text{Er}^{3+}$  distribution profiles overlapped, it is easy for the energy transfer occurring between nearby  $\text{Pr}^{3+}$  and  $\text{Er}^{3+}$ .

The broad emission band ranging from 450 to 700 nm was not affected by the presence of  $\text{Pr}^{3+}$ , which means this PL band was originated from amorphous and c-Si (nc-Si) luminescence in  $\text{SiO}_2$  matrix. Since Er–Pr codoped samples high dose RE ions were implanted in SRSO film ( $[\text{Er}] = 2 \times 10^{20} \text{ cm}^{-3}$ ,  $[\text{Pr}] = 2 \times 10^{20} \text{ cm}^{-3}$ ), above PL performance of  $\text{Pr}^{3+}$  and  $\text{Er}^{3+}$  can be understood as following. High concentration c-Si (nc-Si) provided a large absorption cross-section and acted as sensitizers for the RE ions. It contributed to an efficient route for efficient energy transfer of  $\text{Pr}^{3+}$  and  $\text{Er}^{3+}$ .

In Fig. 3, when the  $\text{Pr}^{3+}$  ion dose was  $4 \times 10^{16} \text{ cm}^{-2}$  with Er/Pr concentration ratio of 1/2, corresponding to  $\text{Pr}^{3+}$  concentration in films up to  $4 \times 10^{20} \text{ cm}^{-3}$ , the PL intensity for RE ions decreased. There is only a weak peak at 495 nm corresponding to  $\text{Pr}^{3+}$   ${}^3\text{I}_0 + {}^3\text{P}_1 \rightarrow {}^3\text{H}_4$  transition. It has been demonstrated the concentration quenching effect happened when high dose of Pr ions were implanted. On the other hand, the PL from RE ions disappeared because of the clustering effect, which decreased the 4f shell emission from trivalent RE ions. The broad emission band ranging

from 450 to 700 nm originated from amorphous and c-Si (nc-Si) in  $\text{SiO}_2$  matrix disappeared. It is proposed that great sputtering effect peeled off the c-Si (nc-Si) in the surface through high dose of Er–Pr ion implantation, and the RE metal layer was formed in the surface of the films. It thus prevented the light emission from c-Si (nc-Si) in  $\text{SiO}_2$  matrix.

#### 4. Conclusions

Er and Pr codoped silicon-rich silicon oxide films were prepared. A broad PL spectrum extending from 450 to 700 nm was obtained for Er–Pr codoped samples with Er/Pr concentration ratio of 1 pumped at 325 nm.  $\text{Er}^{3+}$  was demonstrated to act as sensitizer for  $\text{Pr}^{3+}$  in the codoped films, and the green–red band luminescence has been enhanced by energy transfers from  $\text{Er}^{3+}$  to  $\text{Pr}^{3+}$ . The broad emission band ranging from 450 to 700 nm is proposed to be the contribution of amorphous and c-Si (nc-Si) in  $\text{SiO}_2$  matrix. A metal layer can be formed by the radiation progress which can deteriorate the luminescence. It thus implies that Pr–Er codoped SRSO films is a promising material for application in white light-emitting diode (LED) and field emission displays.

#### Acknowledgments

This work was supported by the National Natural Science Foundation of China (Grant No. 10604003), Beijing Nova Program (Grant No. 2006B15) from Beijing Municipal Science and Technology Commission, and Program of New Century Excellent Talent in University (NCET-07-0045) of China.

#### References

- [1] L.F. Johnson, J.E. Geusic, H.J. Guggenheim, et al., Comments on materials for efficient infrared conversion, *Appl. Phys. Lett.* 15 (48) (1969) 48.
- [2] D.C. Hanna, M.J. McCarthy, I.R. Perry, P.J. Suni, Efficient high-power continuous-wave operation of monomode Tm-doped fibre laser at 2  $\mu\text{m}$  pumped by Nd:YAG laser at 1.064  $\mu\text{m}$ , *Electr. Lett.* 25 (20) (1989) 1365.
- [3] Yu-Ho Won, Ho Seong Jang, Won Bin Im, Duk Young Jeon, Tunable full-color-emitting  $\text{La}_{0.827}\text{Al}_{1.9}\text{O}_{19.09}:\text{Eu}^{2+}$ ,  $\text{Mn}^{2+}$  phosphor for application to warm white-light-emitting diodes, *Appl. Phys. Lett.* 89(23) (2006) 231909.
- [4] P.V. dos Santos, M.T. de Araujo, A.S. Gouveia-Neto, Optical temperature sensing using upconversion fluorescence emission in  $\text{Er}^{3+}/\text{Yb}^{3+}$ -codoped chalcogenide glass, *J. Appl. Phys.* 73 (5) (1998) 578.

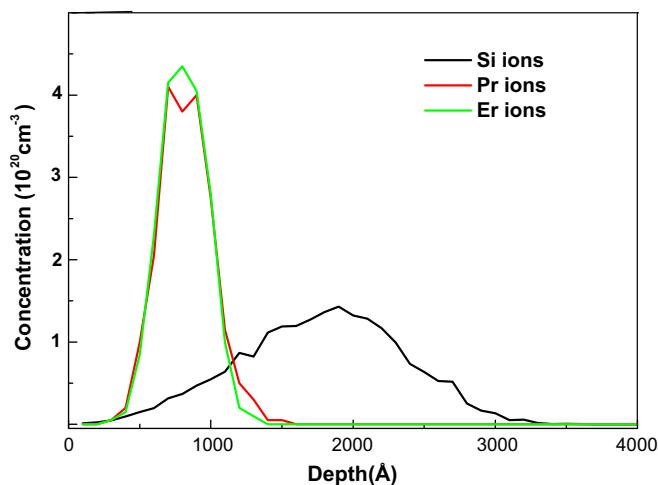


Fig. 5. Concentration profiles of various ions in films simulated by the SRIM2006.

- [5] Y. Dwivedi, A. Rai, S.B. Rai, Intense white upconversion emission in Pr/Er/Yb codoped tellurite glass, *J. Appl. Phys.* 104 (4) (2008) 0435091-4.
- [6] A.S. Gouveia-Neto, L.A. Bueno, R.F. do Nascimento, E.A. da Silva Jr., E.B. da Costa, White light generation by frequency upconversion in Tm<sup>3+</sup>/Ho<sup>3+</sup>/Yb<sup>3+</sup>-codoped fluorolead germanate glass, *Appl. Phys. Lett.* 91 (2007) 091114-3.
- [7] Te-Ju Lee, Li-Yang Luo, et al., Investigation of Pr<sup>3+</sup> as a sensitizer in quantum-cutting fluoride phosphors, *Appl. Phys. Lett.* 92 (8) (2008) 081106-3.
- [8] W. Guo, Y. Lin, X. Gong, et al., Growth and spectroscopic properties of Pr<sup>3+</sup>:NaLa(MoO<sub>4</sub>)<sub>2</sub> crystal, *J. Appl. Phys.* 104 (5) (2008) 053105-8.
- [9] K. Watanabe, H. Tamaoka, M. Fujii, S. Hayashi, Excitation of Tm<sup>3+</sup> by resonant energy transfer from Si nanocrystals, *J. Appl. Phys.* 92 (7) (2002) 4001.
- [10] F. Iacona, G. Franzò, E.C. Moreira, F. Priolo, Silicon nanocrystals and Er<sup>3+</sup> ions in an optical microcavity, *J. Appl. Phys.* 89 (12) (2001) 8354.
- [11] Z. Xiao, F. Xu, G. Cheng, et al., *Phys. Lett. A* 304 (2002) 172.
- [12] M. Wojdak, M. Klik, M. Forcales, O.B. Gusev, et al., Sensitization of Er luminescence by Si nanoclusters, *Phys. Rev. B* 69 (2004) 233315-4.
- [13] P.G. Kik, A. Polman, Exciton–erbium interactions in Si nanocrystal-doped SiO<sub>2</sub>, *J. Appl. Phys.* 88 (4) (2000) 1992.
- [14] M. Perego, S. Ferrari, S. Spiga, E. Bonera, M. Fanciulli, Time of flight secondary ion mass spectrometry study of silicon nanoclusters embedded in thin silicon oxide layers, *Appl. Phys. Lett.* 82 (1) (2003) 121.
- [15] H. Liua, V.S. Vikhnina, L.F. Fonseca, et al., in: *Proceedings of the SPIE*, Vol. 4797, 2003, p. 256.